J. L. Su
M. L. Williams

Noise in Disk Data-recording Media

Abstract: Measurements were made of recording medium noise in erased disks using an in-contact magnetoresistive element and an inductive head supported on an air bearing slider. Four types of coatings on aluminum disks were examined: thin, transition-metal alloy film, CrO_2, FeCo particle, and γ-Fe_2O_3. Results obtained by means of three measurement techniques are in qualitative agreement and indicate that: (1) dc-erased noise of alloy film disks is 14 to 20 dB lower than that of particulate disks measured; (2) dc-erased noise of particulate disks measured is 6 to 16 dB above their bulk-erased noise; (3) although dc noise of particulate disks increases with write current, dc noise of alloy film disks is independent of write current; (4) the shapes of the noise spectra are similar in dc-erased particulate γ-Fe_2O_3 disks and FeCo particle coated disks; and (5) significant modulation noise is detected on particulate disks but not on alloy film disks. The observed dc-erased noise spectrum is compared with the model for small particle noise and is then used to estimate the size of particle agglomerates or voids.

Introduction

Several theoretical and experimental investigations of noise in magnetic tape systems have been published [1-6], but until recently there was little interest in measuring the corresponding noise in disk surface media because it does not limit performance of present disk data storage systems. Disk noise measurements are of theoretical interest because of the relatively well-known head-medium spacing and the expected absence of noise caused by surface irregularities, tape flutter, and inverse magnetostrictive effects associated with head-tape contact. Although most tape noise studies have emphasized the noise of ac-erased media, the emphasis here is on the dc-erased, or uniformly magnetized, state which resembles the saturated digital state. The dc-erase noise provides information about the homogeneity of the magnetic medium, and its measurement can shed light on the suitability of the medium for use at high storage densities. The difference between the observed noise power spectrum and that which would be caused by small particles is interpreted as the noise spectrum of the inhomogeneities. Measurements of particulate coatings, both here and in the literature, indicate higher noise levels for dc erase than for ac erase. For comparison, measurements are presented here of a thin transition-metal alloy film medium, for which the reverse is true.

Techniques of measuring noise spectra

Noise measurements were made on bulk ac-erased and dc-erased disks with an inductive head supported on an air-bearing slider and an in-contact magnetoresistive element. Bulk-erased noise results when the medium has been thoroughly demagnetized by a high-amplitude cyclic field that is spread over a relatively large area. DC erasure reported in this work comprised application of dc current of sufficient amplitude in an inductive write head to saturate the medium. Four types of media coated on aluminum disk substrates were examined: thin alloy film, FeCo particle, CrO_2 and γ-Fe_2O_3. Coating thicknesses are given in Table 1. Three types of measurements were made to obtain narrowband and wideband erased noise spectra.

One type of measurement involves computing the autocorrelation function of erased-noise voltage arising from magnetic media and its Fourier cosine transform to provide noise power-density spectra. The measurement principle is based upon the Wiener theorem: the autocorrelation function of a random function and the power-density spectrum of the random function are related to each other by a Fourier cosine transformation [7]. A magnetoresistive (MR) read element similar to that proposed by Hunt [8] was used to sense fields emanating from erased disks. The element consisted of a thin strip of NiFe film evaporated onto a silicon substrate with its plane perpendicular to the disk surface. A conductor was connected to either end of the strip. The head was mounted on a tripad slider in contact with a slowly rotating (2 to 10 rpm) disk and was connected to a constant-current source, so that the changes in resistivity owing to the fields from the medium could be detected in the form of voltage changes. The autocorrelation function of the MR head output and its Fourier cosine transform were computed from a correlator and a Fourier analyzer, respectively. The output of the Fourier analyzer was connected to an x-y recorder providing noise power-density spectra. This measurement method is limited by the sensitivity and the resolution of the MR head and by the useful frequency range of the correlator, which is from dc to 500 KHz. Slow disk speeds were chosen to operate within the correlator capability and to avoid wear of heads and disks. No thermal spikes [9] caused by the in-contact magnetoresistive head were observed at the speeds tested (0.03 m/s to 0.15 m/s). The MR head was biased in the linear region to obtain maximum bipolar output and the 6 dB resolution of the head was 2500 flux changes/inch (10^5 flux changes/m).

To simulate the functional operation of a disk file, the apparatus for the second type of measurements consisted of an inductive read/write head, a disk drive, read/write electronics and a spectrum analyzer. The disk speed was variable and the speed variation was within 0.3 percent. Measurements were nominally taken at a disk speed of 1260 ips (32 m/s) and at 15 μin. (3.8×10^{-7}m) head-to-disk spacing. The 12-turn head used in this measurement had a track width of 3.6 mils (9.15×10^{-5}m) and a gap length of 54 μin. (1.37×10^{-6}m). The frequency response of the head at the −3 dB point was 8.0 MHz. The spectrum analyzer was used to display the frequency distribution of noise voltages of bulk-erased and dc-erased disks.

The apparatus for the third type of measurements consisted of the same equipment used in the previous measurement except that the spectrum analyzer was replaced by a variable-frequency low-pass Butterworth filter and a true rms voltmeter. Relatively long integration times were used to reduce the error; within 10 seconds the voltmeter reached a final reading that was within 2 percent of a change in the input voltage. The wide-band rms noise voltage, where all frequency components collected at the read head, was measured for various bulk-erased and dc-erased disks.

Measurement of noise spectra

The noise power spectra for γ-Fe_2O_3 disks obtained from the Fourier cosine transform of the autocorrelation function of the MR output are given in Fig. 1 for a disk speed 0.03 m/s. As shown in Fig. 1 the dc-erased noise of γ-Fe_2O_3 disks rises with frequency to a maximum and falls to zero rather rapidly, suggesting that the dc noise is predominant in the long-wavelength region of the spectrum. Repeated measurements on several tracks on various γ-Fe_2O_3 disks indicate similarity in the shape of dc noise power spectra. This result is in good agreement with that obtained by using the inductive head and the spectrum analyzer.

Figure 2 represents the results of measurements using the inductive head, the disk drive, read-write elec-

Table 1 Disk coating thicknesses of various recording media.

Disk	*Coating thickness 0.165-m disk radius* (*m*)	(*μin.*)
γ-Fe_2O_3I	(2.97×10^{-6}).	116
γ-Fe_2O_3II	(1.83×10^{-6}).	72
FeCo particle	(1.78×10^{-6}).	70
CrO_2	(1.52×10^{-6}).	60
Alloy film	[$(2.5 - 5) \times 10^{-8}$].	1 to 2

Figure 1 Representative noise power spectra of particulate γ-Fe_2O_3 disks. Disk speed = 0.03 m/s.

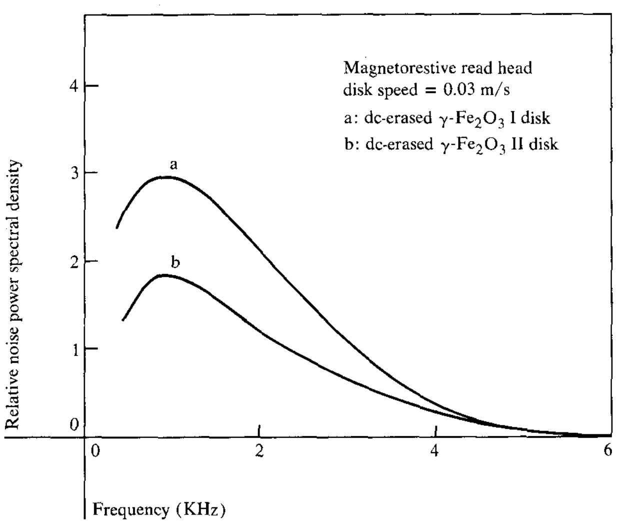

Figure 2 Noise voltage as a function of frequency for bulk-erased and dc-erased disks. Disk speed = 32 m/s, head-to-disk spacing = 3.8×10^{-7}m.

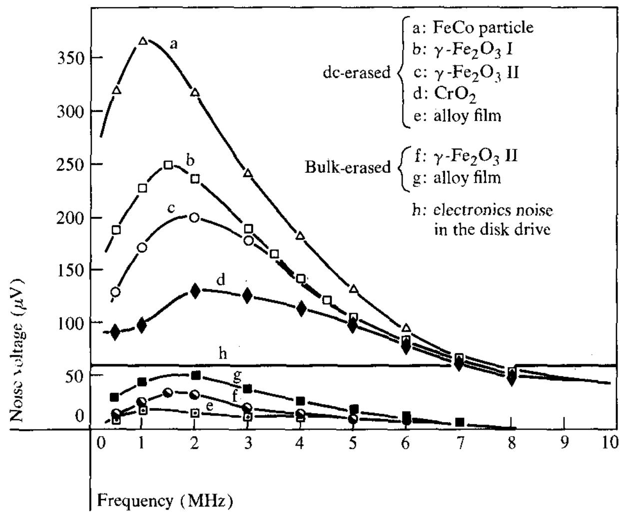

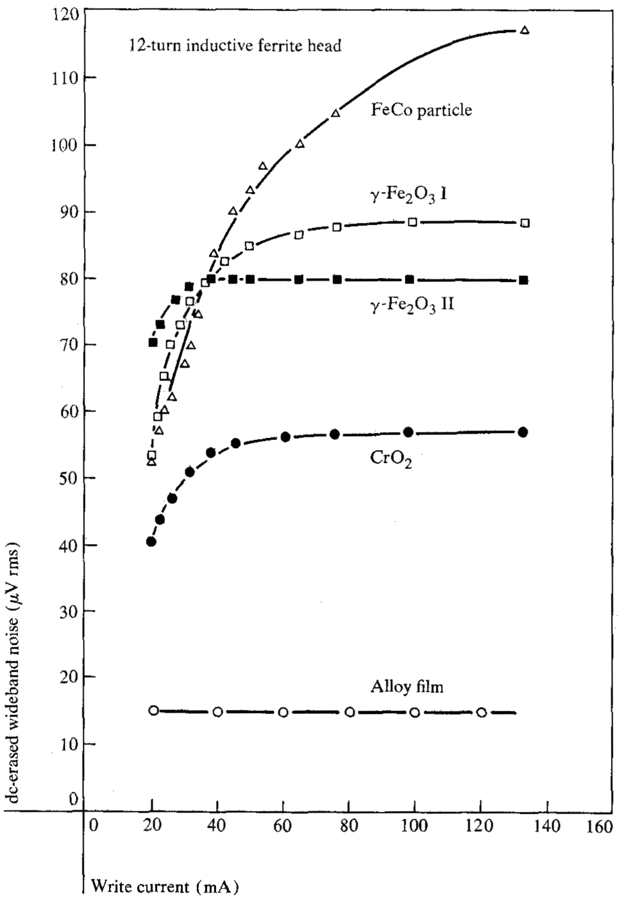

Figure 3 DC-erased wideband noise as a function of write current for various types of media on aluminum disk substrates. Disk speed = 32 m/s, head-to-disk spacing = 3.8×10^{-7}m.

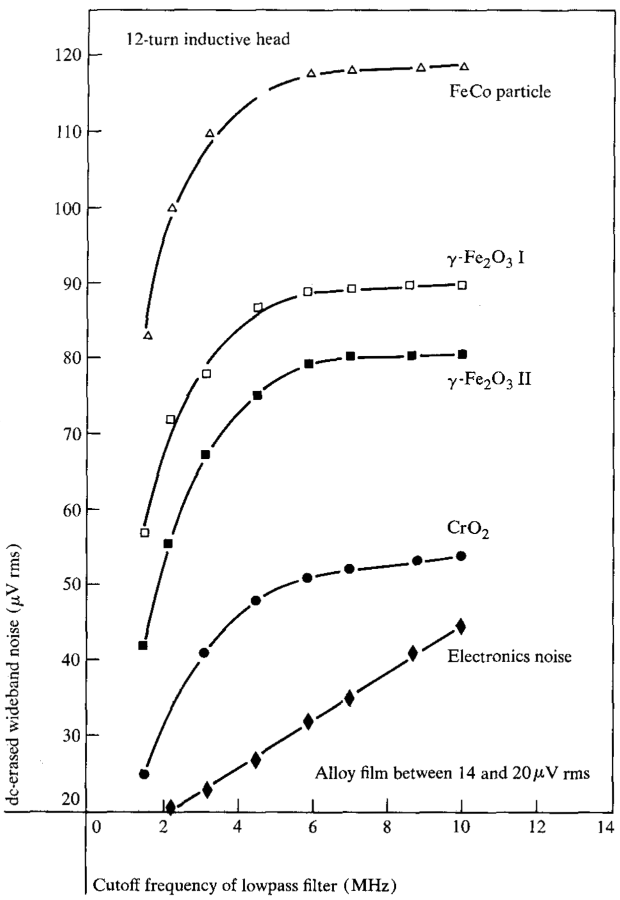

Figure 4 DC-erased wide-band noise as a function of frequency for various types of media on aluminum disk substrates. Disk speed = 32 m/s, head-to-disk spacing = 3.8×10^{-7}m.

tronics and the spectrum analyzer. The noise voltage component is plotted as a function of frequency. Measurements were taken with a 12-turn inductive head spaced 15 μin. (3.8×10^{-7}m) from the disk surface and at a disk speed of 32 m/s. The bandwidth of the spectrum analyzer was set at 30 KHz. For low noise levels, the measurements were repeated employing a 48-turn inductive head and the voltages were scaled to correspond to the 12-turn head data. Electronics noise in the system is also included for comparison. The measured noise levels of dc-erased FeCo particle, γ-Fe_2O_3 and CrO_2 coated disks have a maximum at least one order of magnitude higher than those of bulk-erased disks and dc-erased alloy film disks. As in the previous measurement, the dc-erased noise of particulate disks is seen to be predominant in the long-wavelength portion of the spectrum and decreases rapidly with decreasing wavelengths.

Table 2 Comparison of narrowband noise voltage for various media at 2 MHz and 32 m/s.

(1) Measured head plus electronics noise = 1.7×10^{-9} volts/$\sqrt{Hz}$

(2) DC saturated disk noise at 2 MHz and disk speed = 32 m/s.

Disk	*(Volts/$\sqrt{Hz}$)*	*Relative noise level*
Thin alloy film	3.1×10^{-10}	0.08
CrO_2	3.9×10^{-9}	1
γ-Fe_2O_3II	6.1×10^{-9}	1.57
FeCo particle	9.6×10^{-9}	2.46
γ-Fe_2O_3I	7.4×10^{-9}	1.9

(3) Bulk-erased noise
Alloy film: 1.2×10^{-9} volts/$\sqrt{Hz}$
γ-Fe_2O_3II 9×10^{-10} volts/$\sqrt{Hz}$

Table 3 Isolated pulse amplitude and signal-to-wideband noise ratio for various media.

Disk	*Relative isolated pulse amplitude*	*Wideband S/N ratio Srms at 6 dB/Nrms S/N (total)*	*S/N (medium)*
Alloy film	10.7-14	22-25 dB	36-40 dB
CrO_2	20.7	25.5	30.4
γ-Fe_2O_3II	21.3	23.3	27.2
γ-Fe_2O_3I	27.2	23.1	24.8
Fe-Co particle	13.3	18.1	19.6

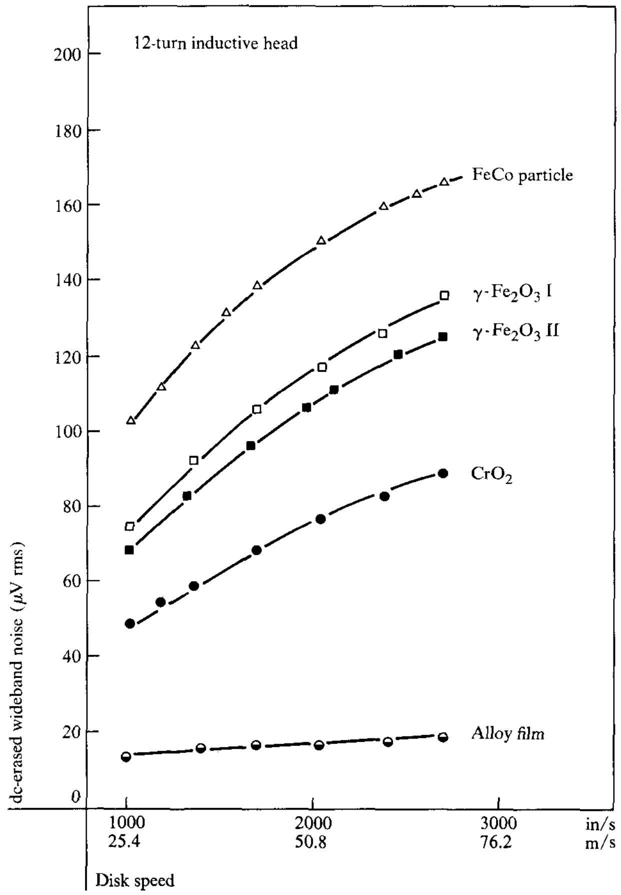

Figure 5 DC-erased wide-band noise as a function of disk speed for various types of media on aluminum disk substrates.

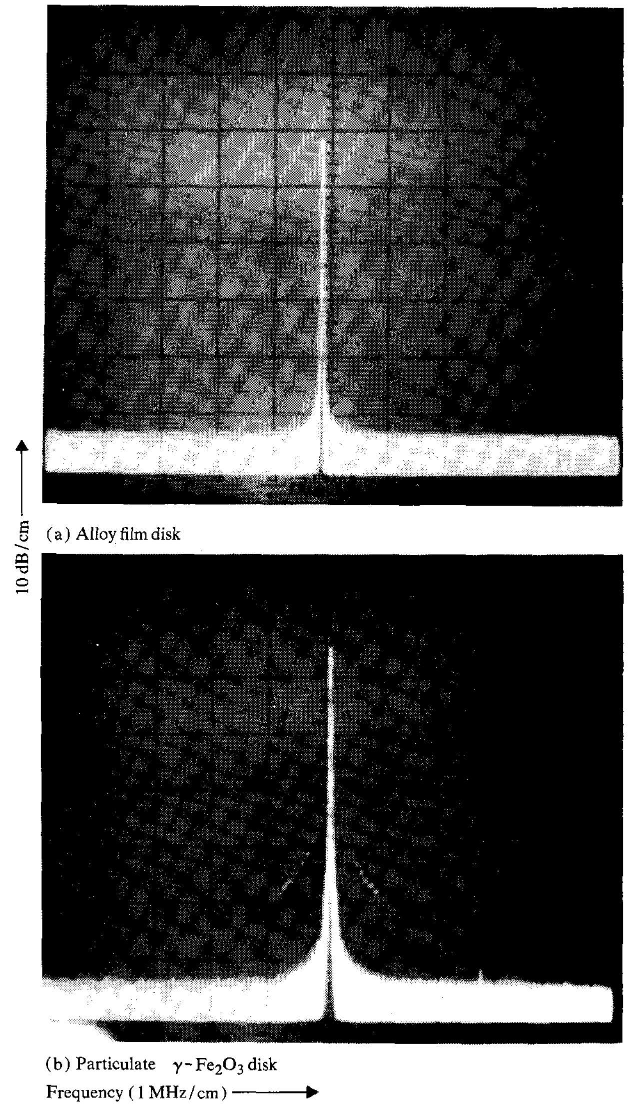

Figure 6 Comparison of modulation noise in alloy film disks and particulate γ-Fe_2O_3 disks. Disk speed = 32 m/s, head-disk spacing = 3.8×10^{-7}m.

A comparison of relative narrowband dc-erased noise levels (at 2 MHz and 32 m/s) for various media is given in Table 2.

The results of wideband noise measurements are presented in Figs. 3, 4 and 5. As shown in Fig. 3, the dc-erased noise of several alloy film disks measured is independent of write current or the magnetization level, and the dc-erased noise of γ-Fe_2O_3, CrO_2, and Fe-Co particle disks increases with increasing write current and saturates at high write current. The frequency dependence of dc saturated noise of various disks is plotted in Fig. 4. The rms noise voltage was measured for different cutoff frequencies of the lowpass filter in the system. The experimental curves for particulate disks in Fig. 4 have much steeper slopes at low frequencies than at high frequencies, indicating the appearance of excessive low-frequency components, which is in agreement with the previous results. Figure 5 shows dc-erased wide-band noise as a function of disk speed. Nonlinearity at high disk speeds results from the increase in the head-to-disk spacing from 12 μin. (3.05×10^{-7}m) at 1000 ips (25.4 m/s) to 23 μin. (5.85×10^{-7}m) at 2800 ips (71.2 m/s).

The signal output and the signal-to-wideband-noise ratio for the disks measured are given in Table 3. The latter was obtained by taking the ratio of the rms voltage of an all-ones signal at −6 dB density and the rms wideband noise voltage.

In Figs. 6(a) and (b) are shown the spectra of an all-ones signal written at −6 dB density for alloy film and particulate γ-Fe_2O_3 disks. A comparison with background noise shows an increase in noise level occurring at frequencies in the vicinity of the written signal frequency, as shown in Fig. 6(b). This modulation noise present only behind the signal is at least 10 dB above the background noise for the case of particulate γ-Fe_2O_3 disks but is barely detectable in alloy film disks.

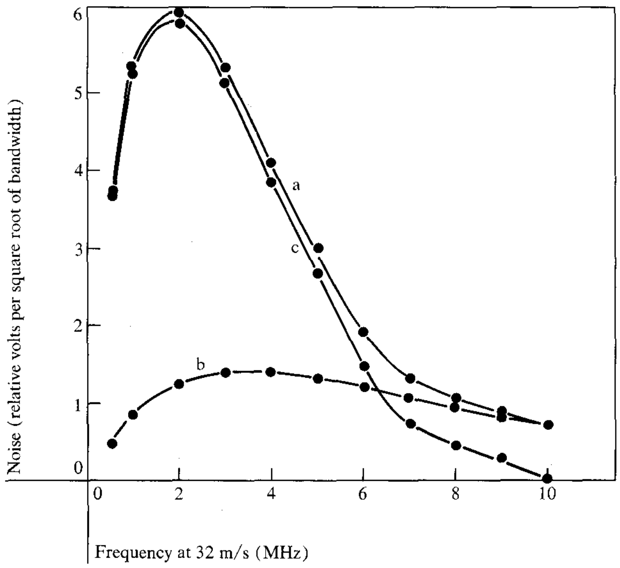

Figure 7 Comparison of observed noise voltage spectrum (a), adjusted small particle contribution (b), and the remaining spectrum (c).

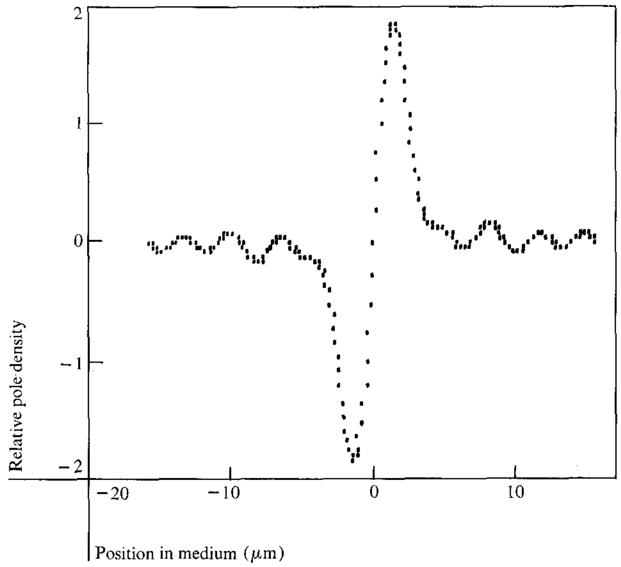

Figure 8 Approximate defect pole distribution derived from data in Fig. 7 as described in the text.

Interpretation of the data

The noise power spectrum of homogeneously, randomly distributed particles, each too small to be resolved by the head, is obtained by adding up the power spectra of the head output resulting from particles at all depths in the medium as done by Mallinson [1], and is of the form

$$E^2(K) = 4\pi (V\mu)^2 nwK \sin^2 (KG/2)(KG/2)^{-2} \times e^{-2KH}[1 - e^{-2KT}], \quad (1)$$

where V is the velocity, $K = 2\pi/\text{wavelength}$, μ is the μ^2 weighted mean particle moment, n is the particle number per unit volume, w is the trackwidth, G is the head gap length, H is the head-to-medium spacing, and T is the coating thickness.

Figure 7 presents typical experimental data and the corresponding calculated small-particle noise, adjusted in amplitude to fit at the high frequencies measured. The observed noise peaks strongly at lower frequencies than the small-particle noise. Also shown is the difference obtained by subtracting the power spectra. The observed noise spectrum at low frequencies consists almost entirely of resolved signals from inhomogeneities in the medium. This permits the measurements to be used for comparing properties of the recording medium.

For inhomogeneities large enough to be resolved, we assume invariance with depth in the coating, so that the pole density spectrum, $P(K)$, is related to the head voltage spectrum $E(K)$ by the relation

$$E(K) = 4\pi V\, P(K)\, K^{-1}[\sin (KG/2)](KG/2)^{-1} \times e^{-KH}[1 - e^{-KT}]. \quad (2)$$

An approximation of the pole density function, $P(X)$, for one of the dominant defects is obtained by taking the odd Fourier transform of $P(K)$. Figure 8 shows the result for the data in Fig. 7. This result resembles the pole density expected from an agglomerate of particles or a void about 3 μm in diameter.

The integrated noise power of large inhomogeneities is about 10 to 20 times that attributable to small particles. For a rough estimate of the fraction of particles this requires to be in agglomerates, we note that this power ratio, R, is roughly $n_a\mu_a^2/n_p\mu_p^2$ where n_a, n_p, μ_a, and μ_p are the number of agglomerates, the number of particles not in agglomerates, the moment of an agglomerate, and the moment of a particle, respectively. If there are A particles per agglomerate, $R = (An_a)A/n_p$ and the fraction of particles in agglomerates is $R/(R + A)$. Using the 3 μm estimated agglomerate diameter, we estimate A to be about 70. This requires that about $\frac{1}{8}$ to $\frac{1}{5}$ of the particles be in agglomerates. The estimate indicates that it is not implausible that there are sufficient agglomerates to explain the noise spectrum observed.

Acknowledgments

We acknowledge the technical assistance of David Longley in instrumentation and data gathering. We are grateful to G. Cheroff for his interest and support.

References

1. J. C. Mallinson, "Maximum Signal-to-Noise Ratio of a Tape Recorder," *IEEE Trans. Magn.* **MAG-5,** 182 (1969).
2. Irving Stein, "Analysis of Noise from Magnetic Storage Media," *J. Appl. Phys.* **34,** 1976 (1963).
3. I. Mikami, "Theory of Noise in Magnetic Recording Tape Coated with Magnetic Particles," *J. Appl. Phys.* **33,** 1591 (1962).
4. E. D. Daniel, "A Basic Study of Tape Noise," Ampex Research Report AEL 1.
5. E. D. Daniel, "A Preliminary Analysis of Surface-Induced Tape Noise," *IEEE Trans. Commun. Electron.* **83,** 250 (1964).
6. D. F. Eldridge, "DC and Modulation Noise in Magnetic Tape," *IEEE Trans. Commun. Electron.* **83,** 585 (1964).
7. Y. W. Lee, *Statistical Theory of Communication*, John Wiley and Sons, New York, 1963.
8. R. P. Hunt, "A Magnetoresistive Readout Transducer," *IEEE Trans. Magn.* **MAG-7,** 150 (1971).
9. R. D. Hempstead, "Thermally Induced Pulses in Magnetoresistive Heads," *IBM J. Res. Develop.* **18,** 547 (1974) this issue.

Received April 1, 1974

The authors are located at the IBM General Products Division Laboratory, Monterey and Cottle Roads, San Jose, California 95193.